Received: 22 December 2023 | Revised: 26 February 2024 | Accepted: 20 March 2024

DOI: 10.1111/mec.17374

ORIGINAL ARTICLE

MOLECULAR ECOLOGY WILEY

Mitonuclear interactions impact aerobic metabolism in hybrids and may explain mitonuclear discordance in young, naturally hybridizing bird lineages

Callum S. McDiarmid[1] | Daniel M. Hooper[2] | Antoine Stier[3,4] | Simon C. Griffith[1]

[1]School of Natural Sciences, Macquarie University, Sydney, New South Wales, Australia

[2]Institute for Comparative Genomics and Richard Gilder Graduate School, American Museum of Natural History, New York, New York, USA

[3]Department of Biology, University of Turku, Turku, Finland

[4]Institut Pluridisciplinaire Hubert Curien, UMR7178, Université de Strasbourg, CNRS, Strasbourg, France

Correspondence
Daniel M. Hooper, Institute for Comparative Genomics and Richard Gilder Graduate School, American Museum of Natural History, New York, NY, USA.
Email: dhooper@amnh.org

Funding information
H2020 Marie Skłodowska-Curie Actions, Grant/Award Number: #894963; Australian Research Council, Grant/Award Number: DP180101783; Gerstner Family Foundation; Holsworth Wildlife Research Endowment; Macquarie University Research Excellence Scholarship

Handling Editor: Michael M. Hansen

Abstract

Understanding genetic incompatibilities and genetic introgression between incipient species are major goals in evolutionary biology. Mitochondrial genes evolve rapidly and exist in dense gene networks with coevolved nuclear genes, suggesting that mitochondrial respiration may be particularly susceptible to disruption in hybrid organisms. Mitonuclear interactions have been demonstrated to contribute to hybrid dysfunction between deeply divergent taxa crossed in the laboratory, but there are few empirical examples of mitonuclear interactions between younger lineages that naturally hybridize. Here, we use controlled hybrid crosses and high-resolution respirometry to provide the first experimental evidence in a bird that inter-lineage mitonuclear interactions impact mitochondrial aerobic metabolism. Specifically, respiration capacity of the two mitodiscordant backcrosses (with mismatched mitonuclear combinations) differs from one another, although they do not differ significantly from the parental groups or mitoconcordant backcrosses as we would expect of mitonuclear disruptions. In the wild hybrid zone between these subspecies, the mitochondrial cline centre is shifted west of the nuclear cline centre, which is consistent with the direction of our experimental results. Our results therefore demonstrate asymmetric mitonuclear interactions that impact the capacity of cellular mitochondrial respiration and may help to explain the geographic discordance between mitochondrial and nuclear genomes observed in the wild.

KEYWORDS
aerobic respiration, cytonuclear discordance, hybridization, mitochondrial, speciation

1 | INTRODUCTION

Understanding the factors that obstruct gene flow or propel genetic introgression between biological lineages is a central goal of speciation research (Coyne & Orr, 2004). One factor that may be particularly susceptible to disruption in hybrids is the interaction between the mitochondrial and nuclear genomes, which underpin mitochondrial aerobic metabolism (Bar-Yaacov et al., 2015; Chou & Leu, 2010; Hill, 2017). Functional mitochondria rely on dense gene networks encompassing genes in both the mitochondrial (N = ~37 genes) and nuclear (N = ~1500 genes) genomes (Figure 1a) (Bar-Yaacov et al., 2012; Hill, 2019a, 2020), and these genes (particularly

mitochondrial genes) can undergo rapid change between lineages (Allio et al., 2017; Mower et al., 2007; Nabholz et al., 2008, 2009; Willett, 2012). Following hybridization, novel combinations of mtDNA and nuDNA may disrupt mitochondrial function and thus act as a reproductive isolating barrier.

Inter-lineage mitonuclear interactions—that is, interactions between the mitochondria of one lineage and the nuclear genome of another lineage that occur within the cells of hybrids—have been demonstrated to contribute to hybrid dysfunction between deeply divergent taxa crossed in the laboratory (Arnqvist et al., 2010; Burton et al., 2013; Ellison et al., 2008; Ellison & Burton, 2008; Montooth et al., 2010). There are, however, fewer empirical examples of inter-lineage mitonuclear interactions between younger taxa that naturally hybridize (Lee et al., 2008; Ma et al., 2016; Moran et al., 2022). In birds, there is suggestive evidence from hybrid zones that mitonuclear incompatibilities may contribute to reproductive isolation based on observed covariation between mitochondrial haplotypes and life history differences or mitonuclear genes (Morales et al., 2018; Toews et al., 2014; Wang et al., 2021). Direct experimental evidence in birds linking hybrid dysfunction with mitonuclear incompatibilities is lacking, however, in large part because most birds cannot be readily kept and bred in captivity. This precludes controlled experiments to effectively disassociate the mitochondrial and nuclear genomes. Naturally produced hybrids that have low physiological function may be compromised for various other reasons, such as their parents mating with a heterospecific because they were poor-quality individuals (Veen et al., 2001). In contrast to genetic incompatibilities of uniform effect on hybrid fitness, interactions of asymmetrical effect (i.e. differential fitness between hybrids based on direction of cross) can result in certain genes introgressing beyond the hybrid zone and geographic discordance between different regions of the genome. In naturally hybridizing systems, geographic discordance between mtDNA and nuDNA is observed at an appreciable frequency but the underlying mechanisms are rarely understood (Toews & Brelsford, 2012). Discordance is often attributed to demographic disparities or sex-biased asymmetries based mostly on verbal arguments (Bonnet et al., 2017), while the functional consequences of mitonuclear interactions such as those described here are rarely considered (Hill, 2019b; Sloan et al., 2017; Toews & Brelsford, 2012).

Optimal function of mitochondrial respiration in birds is dependent on 37 genes in the mtDNA, including 13 protein-coding genes

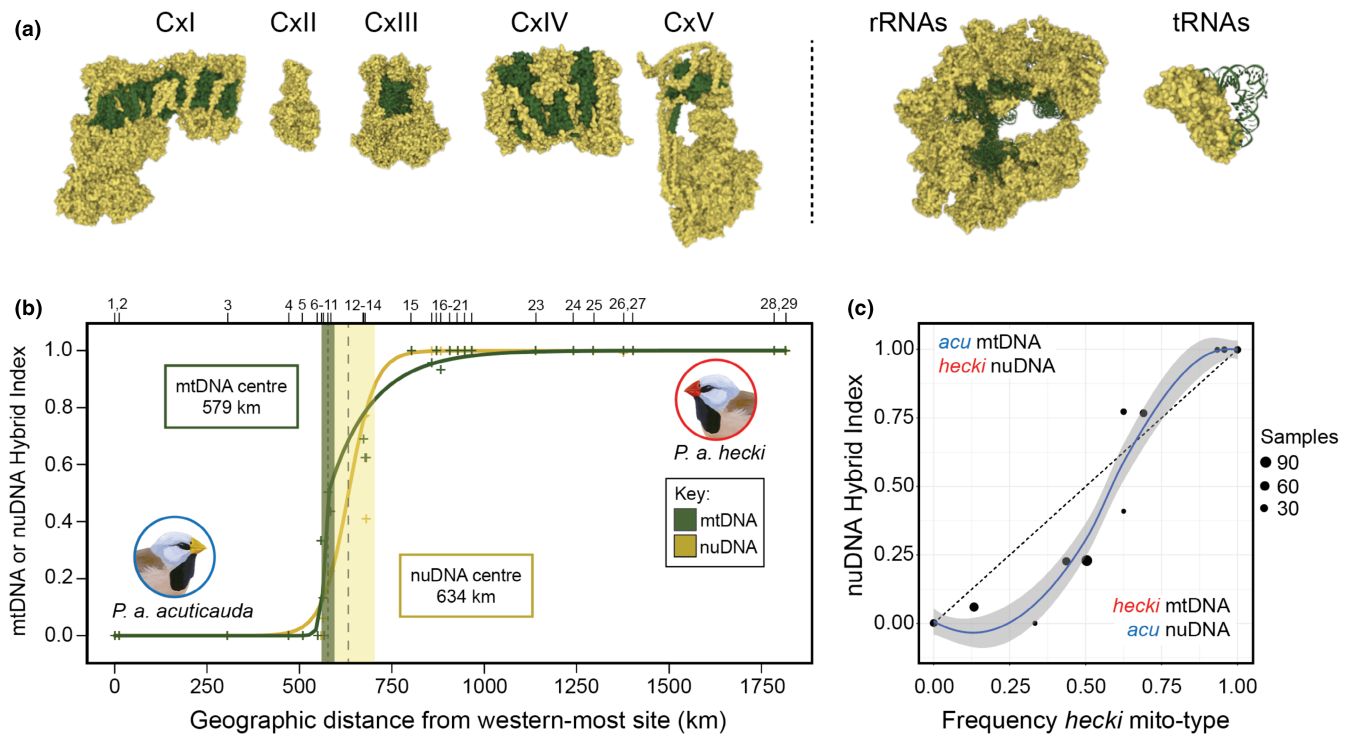

FIGURE 1 Mitochondrial and nuclear genome interactions in the long-tailed finch. (a) Sites of physical interaction within the inner mitochondrial membrane between products encoded by the mitochondrial (green) and nuclear (yellow) genomes. These include proteins that form the electron transport system complexes (CxI-IV) and ATP synthase (CxV), as well as mitochondrial ribosomes and transfer RNA-tRNA synthetases. Complexes are not drawn to scale. The animals and PBD accession numbers for each are CxI (bovine, 5LNK), CxII (chicken, 2H89), CxIII (chicken, 3CWB), CxIV (bovine, 1V45), CxV (bovine, 5ARA—TBC), tRNA (yeast, 4YYE), and rRNA (humans, 3J9M). Figure inspired by Hill et al. 2019. (b) Geographic clines for mtDNA and nuDNA (Z chromosome) across the range of the long-tailed finch. The mtDNA cline centre is 55 km west of the nuDNA cline centre. The position of 29 sampled populations is shown above the panel, and population means for mtDNA and nuDNA are presented as green or yellow crosses, respectively. (c) The frequency of the *hecki* mitotype against nuDNA hybrid index for 11 populations sampled within the hybrid zone, with a loess curve with 95% CI fitted to the data against a dashed line showing the 1:1 neutral expectation. (b) and (c) are based on re-evaluated and re-plotted published data from Lopez et al. (2021) (Lopez et al., 2021).

that encode key components of the well-characterized complexes I, III, IV, and V in the electron transport system (ETS) on the inner mitochondrial membrane. In addition, avian mtDNA encodes two ribosomal RNAs (rRNAs), 22 transfer RNAs (tRNAs), and a control region (OH). In humans, for example, dysfunction of these mitochondrial genes can impact fitness and manifest as mitochondrial diseases and disorders such as neurodegeneration (Hahn & Zuryn, 2019; Stewart & Chinnery, 2015). Changes in the amino acid composition of ETS subunits, or genetic substitutions in the tRNA or rRNA machinery that impact the transcription or translation of ETS subunits, can both potentially destabilize the transfer of high-energy electrons causing them to leak from the ETS. Leaking electrons can contribute to the formation of reactive oxygen species (ROS) that can damage cellular macromolecules (Hahn & Zuryn, 2019).

The subspecies of the long-tailed finch *Poephila acuticauda acuticauda* and *P. a. hecki* inhabit tropical savannahs across northern Australia and naturally hybridize where their distributions meet on the edge of the Kimberley Plateau in Western Australia (Hooper et al., 2019). Previous work has estimated they last shared a common ancestor approximately 0.5 million years ago (0.31–0.68 Mya, 95% HPD) based on divergence in three mtDNA genes (Lopez et al., 2021). Mitonuclear discordance has been observed in the wild hybrid zone between these two subspecies, with the centre of the mitochondrial cline being 55 km west of the nuclear cline centre (Lopez et al., 2021), but within the boundaries of the nuclear hybrid zone (Figure 1b, c, (Lopez et al., 2021)). This discordance suggests that the eastern mitochondrial lineage (mitotype) has introgressed westwards across the hybrid zone. One possible explanation for this apparent introgression is that hybridization could cause novel mitonuclear interactions that asymmetrically reduce the fitness of individuals with a western mitotype and eastern nuclear genome, by adversely impacting aerobic metabolism and therefore ATP synthesis, or through elevated generation of reactive oxygen species (ROS) that results in oxidative stress. The long-tailed finch can be readily kept and bred in captivity, making it an experimentally tractable model system in which to examine the consequences of this potential mitonuclear mismatch.

Here, we test whether inter-lineage mitonuclear interactions impact aerobic metabolism using subspecies of the long-tailed finch. We utilized a crossing strategy designed to expose inter-lineage mitonuclear interactions between the subspecies in the resulting hybrid embryos. We then assessed mitochondrial aerobic respiration capacity using high-resolution respirometry (Koch et al., 2021).

2 | METHODS

2.1 | Study species

Long-tailed finches of each subspecies (*Poephila acuticauda acuticauda* and *P. a. hecki*) used in this study came from captive populations maintained at Macquarie University in Sydney, Australia. Wild-caught *P. a. acuticauda* individuals were originally sourced from Mount House (17°02′ S, 125°35′ E) and Nelson's Hole (15°49′ S, 127°30′ E) in Western Australia, and wild-caught *P. a. hecki* were sourced from October Creek (16°37′ S, 134°51′ E) in the Northern Territory (Brazill-Boast et al., 2011; Rowe et al., 2015). As individuals from these populations show no evidence of genomic admixture between subspecies (Hooper et al., 2019; Lopez et al., 2021), we hereafter refer to them as 'parental'.

2.2 | mtDNA comparison between subspecies

Changes in the mitochondrial genome are required but not sufficient for inter-lineage mitonuclear incompatibility. Even a single substitution in the mtDNA can lead to reproductive isolation (e.g. (Meiklejohn et al., 2013)). To identify substitutions with the potential to contribute to incompatibilities, we sequenced whole mitochondrial genomes from each long-tailed finch subspecies and counted the number of fixed differences and associated amino acid changes within 13 protein-coding genes between them. We assembled mitochondrial genomes using whole-genome sequence (WGS) data from both long-tailed finch subspecies (*P. a. acuticauda*, $N = 14$; *P. a. hecki* $N = 11$) and their sister species the black-throated finch *P. cincta atropygialis* ($N = 11$; Table S1). We used bcftools (version 1.9) (Li, 2011) consensus after calling and incorporating variants relative to the zebra finch reference genome (GCA_003957565.4) in each sample. Ambiguous positions were output with associated IUPAC codes (Martindale & Holbrook, 2002). We exclusively used WGS data derived from DNA extracted from muscle (rather than blood) to ensure that they were enriched for reads from mitochondrial DNA and not reads from the nuclear-encoded mtDNA (NUMT) copy. The mitochondrial genome of the zebra finch reference was used as an additional outgroup to help assign substitutions to their lineage of origin. We used the MITOS2 WebServer (Donath et al., 2019) to extract specific sequences for each mtDNA-encoded gene, including all 13 protein-coding genes, 22 tRNA, and 2 rRNA and the control region. Each gene was aligned using MAFFT (version 7) web aligner (Katoh et al., 2017), and we manually examined each alignment with Geneious prime (version 2023.1.2) to count and characterize the distribution of fixed differences between each of the three members of *Poephila* (Table S2). For each protein-coding gene, we calculated the average level of sequence divergence between taxa (D_{XY}) using the program DnaSP (version 6 (Rozas et al., 2017)).

We next evaluated the extent of non-synonymous change between long-tailed finch subspecies for each protein-coding gene. We generated lineage-specific consensus sequences for each gene and used the vertebrate mitochondrial genetic code to translate these to amino acid sequence. We again used data from the black-throated finch and zebra finch as outgroups to assign amino acid changes to the long-tailed finch subspecies of origin. We classified each amino acid substitution by any associated change in biochemical properties. Finally, we calculated the ratio of the rate of non-synonymous to the rate of synonymous nucleotide substitutions (dN/dS) between long-tailed finch subspecies for each

protein-coding gene using the model M0 implemented in the program Easy-CodeML (v1.41) (Gao et al., 2019).

2.3 | Breeding

Embryos were produced by rotating pairs of long-tailed finches through 20 outdoor aviaries (4.1 m long × 1.85 m wide × 2.24 m high), with one pair per aviary containing nest boxes and nesting material. Mealworms, greens, dry seeds, and water were provided ad libitum. We required females to have been exclusively with the partner for 14 days minimum before any experimental eggs were collected, to avoid embryos being sired by stored sperm from a different male. Nest boxes were checked every day, and eggs were collected the day they were laid, given a unique number using a permanent marker, and stored in a 'soft box' at cool room temperature (22°C) for up to 7 days before being placed into an incubator (Brinsea Ovation 56 EX, Brinsea Products, Winscombe, UK). Eggs were incubated at 37.5°C and 65% humidity for 12 days. On the 12th day (i.e. the day before expected hatch), eggs were removed and measurements made. Working with embryos meant we eliminated the opportunity for the effects of extended parental care by parents of different genetic backgrounds.

2.4 | Crossing design

We produced backcrossed offspring by first breeding F_1 hybrid females with an unadmixed parental male of each subspecies, sequentially and in random order. Resulting offspring were defined as 'mitoconcordant' backcrosses if their father's lineage *did* match their mother's mitotype and were defined as 'mitodiscordant' backcrosses if father's lineage *did not* match their mother's mitotype (Figure 2). We note that in the literature these groups are often referred to as 'maternal' and 'paternal' backcrosses, respectively. Parental pairs of each subspecies were set up to breed at the same time and used as controls.

Mitodiscordant backcrossing exposes incompatibilities by producing offspring who inherit most of their nuclear genome from a different lineage than that of their mitochondrial genome. This is particularly pronounced in the case of the long-tailed finch, as >98.5% of fixed nuclear differences between subspecies are on the Z chromosome (Singhal et al., 2015). In our cross design, mitodiscordant backcross offspring inherit Z chromosomes that have had no opportunity for recombination between subspecies. If male, they receive one Z chromosome from their hemizygous F_1 mother and a Z chromosome of matching subspecies identity from their father. Females have only a single Z chromosome inherited from their father. Mitodiscordant backcrosses not only have mismatched mitochondrial and nuclear genomes but also have a low level of admixture on autosomes in their nuclear genome, which would otherwise be a potentially confounding source of hybrid dysfunction. For this reason, we included mitoconcordant backcross individuals as controls, as their level of autosomal admixture is the same as mitodiscordant backcrosses, but their mitochondria and Z chromosomes come from the same subspecies (Figure 2). It is worth noting that these several different types of backcrossed hybrids are also highly relevant to the wild hybrid zone, where we previously described that ~68% (243 of 357) of individuals had some level of admixture (Lopez et al., 2021).

The goal of our cross design was to create embryos in which the mitochondrial haplotype (i.e. mitotype) of the two subspecies was placed in three distinct contexts: (1) a nuclear genetic background exactly matching the mitotype lineage (parental crosses), (2) a nuclear genetic background mostly matching the mitotype lineage (mitoconcordant backcrosses), and (3) a nuclear genetic background mostly not matching the mitotype lineage (mitodiscordant backcrosses). The six resulting groups of embryos were thus (1) parental *acuticauda* (*acuticauda* mother × *acuticauda* father), (2) parental *hecki* (*hecki* mother × *hecki* father), (3) mitoconcordant backcross *acuticauda* (F_1 mother with *acuticauda* mtDNA × *acuticauda*

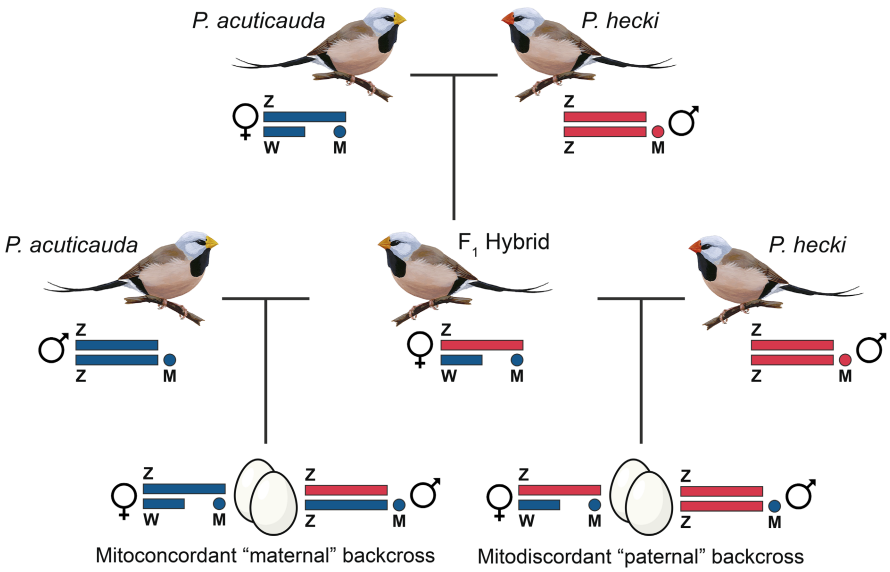

FIGURE 2 Experimental design used to breed mitoconcordant maternal and mitodiscordant paternal backcross offspring. The example shown represents the cross between *P. a. acuticauda* females and *P. a. hecki* males used to generate mitoconcordant (i.e. maternal) and mitodiscordant (i.e. paternal) backcross hybrids carrying *acuticauda* mitotypes. The reciprocal cross used to generate *hecki* mitotype carrying backcross hybrids was structured in the same way.

father), (4) mitoconcordant backcross *hecki* (F_1 mother with *hecki* mitotype × *hecki* father), (5) mitodiscordant backcross *acuticauda* (F_1 mother with *acuticauda* mtDNA × *hecki* father), and (6) mitodiscordant backcross *hecki* (F_1 mother with *hecki* mtDNA × *acuticauda* father). Mothers used in parental crosses only produced a single clutch, while F_1 hybrid mothers used for backcrossing usually produced two clutches: one with an *acuticauda* father and one with a *hecki* father (however, four F_1 females only produced a clutch with one partner). All fathers were only used for a single clutch.

2.5 | Heart rate measurement

After 12 days of incubation, each egg was removed from the incubator and immediately placed on a Buddy digital egg monitor (Vetronic Services, Abbotskerswell, Devon, UK), to measure embryonic heart rate from within the egg (a proxy for whole-body metabolic rate) (Sheldon et al., 2018). A timer was started when the egg was removed from the incubator, and heart rate and corresponding time since removal were recorded at least twice over 2 min. We used these measurements to calculate the rate of cooling and the predicted heart rate halfway through the period (i.e. at 60 s). Five individuals whose heart rate was only measured once were excluded from this dataset.

2.6 | High-resolution respirometry strategy

High-resolution respirometry was performed with permeabilized tissue samples from these embryos using an Oroboros O2k (Oroboros Instruments, Innsbruck, Austria). High-resolution respirometry allowed us to systematically stimulate, uncouple, and inhibit certain combinations of mitochondrial complexes (Table 1; Figure S1). The biochemistry and genetic architecture underlying the core proteins of oxidative phosphorylation (OXPHOS) is highly conserved across eukaryotes and has been well described (Burton et al., 2013; Hill et al., 2019) with four protein complexes (CxI, CxII, CXIII, and CxIV) establishing the proton gradient across the mitochondrial membrane, and CxV driving ATP synthesis (see also Figure 1). We measured the maximum capacity of OXPHOS system when fuelled by electrons either through complex I (CxI) or both CxI and CxII in tandem (OXP-I, OXP-I,II), and the maximum capacity of the ETS when accepting electrons from CxII, and both CxI and II in tandem (ETS-I,II, ETS,II). Comparing our experimental groups for these measures reveals whether CxI is compromised. We also assessed the maximum capacity for complex IV in isolation to consume O_2, a measure not reliant on CxIII, which can reveal if CxIII is compromised. We also quantified the component of respiration that is not available to fuel ATP synthesis (LEAK-I,II).

These measures enable us to test whether mitonuclear interactions impact mitochondrial aerobic metabolism in long-tailed finch hybrids. More specifically, they allow us to interrogate the source of any mitonuclear dysfunction, be it from the two complexes with amino acid differences between subspecies (CxI and III) or from translational issues related to fixed differences in the mtDNA-encoded tRNAs or rRNAs (Birben et al., 2012; Marasco et al., 2017; Martindale & Holbrook, 2002).

2.7 | High-resolution respirometry technical steps

After the embryonic heart rate was measured, embryos were used for high-resolution respirometry. Embryos were euthanized via decapitation and then weighed (Mettler Toledo, PB303-S/FACT, Colombus, Ohio, USA). There was no significant difference between experimental groups in embryonic survival ($X^2_5 = 4.1$, $p = .53$; Figure S3B) or mass at day 12 of incubation ($X^2_5 = 7.3$, $p = .20$; Table 2; Figure S3C). The head and body were then laterally cut into two, and the right-hand side was placed in 400 µL of phosphate-buffered saline (PBS), homogenized with three strokes of a teflon9-glass Potter–Elvehjem homogenizer (Wheaton, 5 mL), and stored at −80 for later analyses including DNA extraction for sex determination (described below). The left-hand side was weighed, suspended in a dilution of 100 mg/mL of MiR05 medium

TABLE 1 Mitochondrial respiration metrics.

Respiration measure	Description of measure	ETS complex included in each measure	Repeatability (SE) from 40 samples run in duplicate
OXP-I,II	Coupled respiration	I, II, III, IV, V	0.94 (0.02)
ETS-I,II	Uncoupled respiration	I, II, III, IV	0.90 (0.03)
OXP-I	Coupled respiration	I, III, IV, V	0.69 (0.09)
ETS-II	Maximum capacity of the ETS	II, III, IV	0.96 (0.01)
CxIV	Maximum respiration	IV	0.93 (0.02)
LEAK-I,II	Respiration linked to proton leak	I, II, III, IV	0.89 (0.03)

Note: The high-resolution respirometry measures used in this study to assess mitochondrial function, the electron transport system (ETS) complexes involved, and the repeatability of each based on the 40 samples run in duplicate.

TABLE 2 Mitochondrial protein-coding divergence between long-tailed finch subspecies.

Complex	Gene	Fixed differences	D_{XY}	dN/dS
Complex I	*NAD1*	12	0.014	0.0001
	NAD2	8	0.017	0.0001
	NAD3	3	0.009	0.1142
	NAD4	9	0.010	0.0599
	NAD4L	5	0.018	0.0001
	NAD5	17	0.011	0.0127
	NAD6	17	0.029	0.0210
Complex III	*COB*	10	0.009	0.0574
Complex IV	*COX1*	9	0.009	0.0001
	COX2	4	0.006	0.0001
	COX3	3	0.005	0.0001
Complex V	*ATP6*	10	0.017	0.0001
	ATP8	0	0.001	0.0001
Combined		**107**	**0.010**	**0.0168**

Note: The 13 protein-coding genes comprising the electron transport system (ETS) are organized by complex. Fixed differences and the average number of nucleotide substitutions per site between subspecies (D_{XY}) were inferred based on comparison of full mitochondrial genomes of *Poephila a. acuticauda* ($N = 14$) and *P. a. hecki* ($N = 11$). Estimates of dN/dS were calculated for each gene using the model M0 implemented in the program Easy-CodeML (v1.41; Gao et al. 2019). The combined estimate of dN/dS was inferred based on net dN (0.0114) and dS (0.6802) across all protein-coding genes. A full list of substitutions within sampled members of *Poephila* is available in Table S2.

Values in bold represent a results of all genes combined.

(0.5 mM Egtazic Acid (EGTA), 3 mM $MgCl_2$, 50 mM K-lactobionate, 20 mM taurine, 10 mM KH2PO4, 20 mM Hepes, 110 mM sucrose, free fatty acid bovine serum albumin (1 g L-1), pH 7.1; (Stier et al., 2017; Ton et al., 2021)), and then homogenized and mechanically permeabilized using a teflon-glass Potter–Elvehjem homogenizer (Wheaton, 5 mL). All work was done on ice. This homogenate was centrifuged for 1 min at 100*g* to pellet big tissue, and then 500ul of the supernatant was added to a chamber of an Oroboros O_2k high-resolution respirometer set at 37°C. The respirometer had two chambers, and we always ran two samples in parallel. After two samples were loaded and the system had equilibrated (oxygen consumption was stable), 2 µL of digitonin (10 mg/mL) was added to ensure cells were fully permeabilized. We injected 5 µL pyruvate (5 mM final), 5 µL malate (2 mM final), 10 µL glutamate (10 mM final) as electron donors for CxI, and then measured oxidative phosphorylation when only CxI was receiving electrons (OXPHOS-I) by adding 5 µL adenosine diphosphate (ADP, 1.25 mM final). We next measured coupled respiration capacity through both CxI and II (OXPHOS-I,II) by adding 25 µL succinate (10 mM final). We then determined O_2 consumption associated with proton leak when electrons were being received by both CxI and II (LEAK-I,II) by adding 5 µL oligomycin (10 µM final). We next estimated the maximum capacity of the electron transport system (ETS-I,II) by titrating the mitochondrial uncoupler carbonyl cyanide m-chlorophenyl hydrazine (CCCP; at 2 mM concentration) by first one injection of 3 µL, followed by 1 µL steps. We next estimated the ETS capacity when only receiving electrons through CxII (ETS-II) by adding 1 µL rotenone (0.5 µM final). We then measured non-mitochondrial O_2 consumption by injecting 1 µL of antimycin A (2.5 µM final) to inhibit CxIII. Finally, we estimated the respiration capacity of CxIV directly by first adding 5 µL TMPD (0.5 mM final) and 5 µL ascorbate (2 mM final), and then calculating the background chemical respiration rate by adding 50 µL azide (100 mM final). Across all runs the chambers were opened consistently at the same stages for reoxygenation. After each run, 1 mL of the solution was taken from each respirometer chamber and frozen at −80°C, and at the conclusion of all measures we performed a Pierce BCA protein quantification assay on this stored solution (ThermoFisher, Scientific, Waltham, MA, USA). Protein quantity was included as a covariate in statistical models (below) to account for slight differences in the amount of biological material in each sample. In most cases, a different embryo sample was run in each chamber, but in 40 cases the same embryo was run in duplicate to assess how repeatable these measurements were (Table 1). When two different samples were run, the first was sitting in the respirometer for some time before the protocol was begun, and to account for any variability introduced by this we included a covariate in our models that was the length of time between when the embryo sample entered the chamber and when the measure was made.

2.8 | Molecular sexing

We extracted DNA from the homogenized right side of all embryos using a Gentra PureGene kit (Qiagen, Valencia, CA, USA) following manufacturer instructions. We sexed embryos by amplifying an intronic portion of the CHD gene that differs in size between the Z-linked and W-linked copy following published protocols (Lee et al., 2010; Lopez et al., 2021). Gel electrophoresis of the PCR product revealed the sex of the embryo as either male (one band, homozygous, ZZ) or female (two bands, heterozygous, ZW).

2.9 | mtDNA copy number

We estimated mitochondrial density based on mtDNA copy number for all samples using real-time quantitative PCR (qPCR) analysis following protocols established for passerine birds (Stier et al. 2019, Stier et al. 2022). While the amount of mtDNA in a mitochondrion can vary, mtDNA copy number is a reliable proxy of mitochondrial density. We estimated the relative mtDNA copy number by measuring the amount of mtDNA relative to the nuDNA for each sample by qPCR on a CFX96 Real-Time System (BIO-RAD). We used RAG1 as a representative single-copy nuclear gene (F: GCAGATGAACTGGAGGCTATAA,

R: CAGCTGAGAAACGTGTTGATTC) and used COX1 as our representative mitochondrial gene (F: TCCTAGCCAACTCCTCAC, R: CCTGCTAGGATTGCAAAT). A complete nuclear copy of the mitochondrial genome (i.e. a NUMT) exists in Estrildid finches, for example, in the zebra finch reference genome (GCA_003957565.4) at chr2:72232845–72249691. To minimize the risk of NUMT interference in estimating mtDNA copy number, we designed our COX1 primers to perfectly match the mitochondrial sequence observed in *Poephila*. Moreover, our use of embryo tissue is less likely to result in amplification of the NUMT as gDNA from muscle tissue has a much lower nuclear: mitochondria ratio than gDNA from blood (Sorenson & Quinn, 1998). We further verified that COX1 amplification resulted in a single product of the expected size on an agarose gel.

Following Stier et al. (2022), qPCR reactions had a total volume of 12 μL that included 6 ng of DNA and had PCR primers with concentrations of 200 nM and 6 μL of Absolute Blue qPCR Mix SYBR Green low ROX (Thermos Scientific). The qPCR conditions were 15 min at 95°C, 40 cycles of 15 s at 95°C, 30 s at 58°C, and 30 s at 72°C. Samples were run in triplicate for each gene (RAG1 and COX1) across five plates, ten samples were pooled and included on every plate as a reference, and 20 samples were included on two separate plates. Amplicon efficiency was estimated from a standard curve of the reference between 1.5 and 24 ng (1.5, 3, 6, 12, 16, 24) run on one plate. The mean reaction efficiencies were 92.1% for RAG1 and 82.3% for COX1. To calculate relative mtDNA copy number for each sample, we used the following formula: $(1+Ef_{COX1})^{\Delta CqCOX1}/(1+Ef_{RAG1})^{\Delta CqRAG1}$, with Ef as the amplicon efficiency, ΔCq as the difference in Cq between the reference and focal samples. Some samples were run twice on separate plates, with an inter-plate repeatability of 0.74 (95% CI [0.49, 0.88]), and based on triplicates intra-plate repeatability was 0.94 (95% CI [0.93, 0.95]). Seven samples were considered outliers (Cq RAG1 < Cq COI) and removed from analysis.

2.10 | Oxidative damage assay

It is possible that some aspect of mitochondrial function other than aerobic respiration is impaired, but that the respiration rate is maintained. For this reason, we also measured the damage induced by reactive oxygen species (ROS). High ROS levels resulting from mitochondrial dysfunction can damage macromolecules, cell components, and structures (Birben et al., 2012; Martindale & Holbrook, 2002), and ROS-induced DNA damage correlates with shorter lifespan in the closely related zebra finch (Marasco et al., 2017). 8-OHdG (8-hydroxy-2′-deoxyguanosine) is a predominant form of ROS-induced oxidative lesions to genomic DNA that has been widely used as a biomarker for oxidative damage (Valavanidis et al., 2009) and has been associated with increased mitochondrial respiration in birds (Stier et al., 2019, 2022). While 8-OHdG does not block DNA replication, it contributes to mutagenesis and can affect DNA transcription (Markkanen, 2017). Here, we quantified levels of 8-OHdG in the DNA extracted from embryos using a competitive immunoassay (300 ng DNA, EpiQuick 8-OHdG DNA Damage Quantification Direct Kit Colorimetric, Epigentek, USA) following the manufacturer recommendations. This was run on a subset of samples ($N = 182$) chosen blind to respiration capacity to have roughly balanced numbers from each experimental group ($N = 28–33$ samples per group). The intra-plate coefficient of variation based on duplicates was 6.3 ± 0.83. The inter-plate coefficient of variation based on four samples repeated over all three plates was 22.7 ± 4.05, so we included plate ID as random effect in our analyses.

2.11 | Statistical analyses

For statistical analyses, we used R version 4.1.2 (R Core Team, 2020) using RStudio version 1.2.5033 (RStudio Team, 2020) for the graphical interface. We used the lme4 and lmerTest packages (Bates et al., 2015; Kuznetsova et al., 2017) to run linear mixed models to test whether our measures of respiration capacity differed between the six experimental groups (parental *acuticauda*, parental *hecki*, mitoconcordant and mitodiscordant backcross with *acuticauda* mtDNA, mitoconcordant, and mitodiscordant backcrosses with *hecki* mtDNA). These measures were each included as the dependent variable in separate linear mixed models, in which the fixed effects were experimental group, embryo sex, protein quantity in the chamber, and the length of time after embryo entered the oroboros chamber when the measure was made. In each, we tested for an interaction between experimental group and embryo sex, and if this was not significant the interaction term was removed (but left in the model if significant). In each model, parental pair ID was included as a random effect, to account for multiple members of the same clutch being included. Where there was a significant effect of experimental group, we ran Tukey's post-hoc comparisons using the emmeans package (Lenth, 2020) to assess specifically which groups differed from one another. Model assumptions were checked using the DHARMa package in R (Hartig, 2021).

We similarly ran linear mixed models to test whether heart rate, oxidative damage, and mitochondrial copy number differed between our experimental groups, but in these cases the fixed effects were experimental group, embryo sex, and for the heart rate model embryo mass, and the random effect was still parental pair ID. Oxidative damage and mitochondrial copy number were log transformed to better meet model assumptions. An interaction between experimental group and sex was also included for each model, but then removed if not significant. In the mitochondrial copy number and oxidative damage models, plate ID were additionally included as random effects. Embryo ID was also initially included as a random effect in the mitochondrial copy number and oxidative damage models, but it explained close to zero variance so was removed for the final models, likely because very few individuals were measured twice (10 for mitochondrial copy number, 21 for oxidative damage). A small number of values for mitochondrial copy number were extremely high ($N = 10$, total $N = 211$), well above the normally distributed other samples and were likely technical errors, and so were excluded to facilitate modelling.

3 | RESULTS

We found a low level of divergence in mtDNA between subspecies, with fixed differences observed in only 0.9% of positions comprising the protein-coding genes of the electron transport system (107 of 11,361 bp total; Table 3). The average nucleotide divergence per site (D_{XY}) was highly variable, however, across protein-coding genes, ranging from 0.1% (ATP8) to 2.9% (NAD6), and between complexes: divergence was 2.1-fold higher on average for genes in complex I than in complex IV (Table 3). We observed a total of seven fixed amino acid differences between subspecies, five differences in four genes in complex I, and two amino acid differences in the cytochrome b (COB) gene in complex III. There were no amino acid differences between the subspecies in either complex IV or complex V. The inferred mitochondrial genome-wide dN/dS ratio between long-tailed finch subspecies is well below 1 at 0.0168, suggesting that purifying selection is the dominant force shaping mitochondrial evolution in *Poephila* (Table 3). Of the five genes with observed non-synonymous differences between subspecies, dN/dS ranged from 0.0127 (*NAD5*) to 0.1142 (*NAD3*).

In the non-coding region, we observed a further six fixed differences between subspecies in the small and large rRNA genes (four and two differences, respectively) and a total of four fixed differences in four mitochondrial tRNAs (Table S2). These non-coding differences provide additional potential sites of mitonuclear incompatibilities that could impact mitochondrial function via the transcription, translation, or replication of mtDNA (e.g. [41]). On the other hand, any protein–protein mitonuclear incompatibilities in this system should be restricted to impacting the function of complexes I or III.

Polarization inference from the use of outgroup taxa revealed that of the seven fixed amino acid differences between subspecies, six have occurred in the *hecki* lineage (Figure 3; Table 4). Three of the amino acid substitutions derived within *hecki*, and the single amino acid change derived in *acuticauda*, result in a change from a polar to a non-polar amino acid (Table 4). In the non-protein-coding genes (rRNAs, tRNAs, OH), there was a roughly even spread of derived DNA sequence changes between lineages (6 *acuticauda* and 4 *hecki*, Tables S2 and S4).

We observed a significant difference between the two mito-discordant backcross groups for all five measures of aerobic respiration capacity (except borderline non-significant for females for OXP-I,II, $p = 0.064$), whereby individuals with *acuticauda* mtDNA and *hecki* nuDNA had lower respiration capacity than did individuals with *hecki* mtDNA and *acuticauda* nuDNA (Table 5; Figure 4, Figure S2). There were no other differences between experimental groups that were as consistent across the five measures of aerobic capacity we measured (Table 5). For the measure ETS-I,II, the

TABLE 3 mtDNA amino acid differences between long-tailed finch subspecies.

Complex	Gene	Mutation	Biochemical change	Origin
Complex I	*NAD3*	T9A	Polarity change (+ > −)	*Hecki*
	NAD4	T96A	Polarity change (+ > −)	*Hecki*
	NAD4	T398A	Polarity change (+ > −)	*Hecki*
	NAD5	A16V	None	*Hecki*
	NAD6	S127L	Polarity change (+ > −)	*Acuticauda*
Complex III	*COB*	S358T	None	*Hecki*
	COB	I372M	None	*Hecki*

Note: Fixed differences were assigned to their lineage of origin using mitochondrial genomes of the black-throated finch (*Poephila cincta atropygialis*; $N = 11$) and the zebra finch (*Taeniopygia guttata*; $N = 1$) as outgroups. A full set of amino acid substitutions between sampled members of Poephila are reported in Table S4.

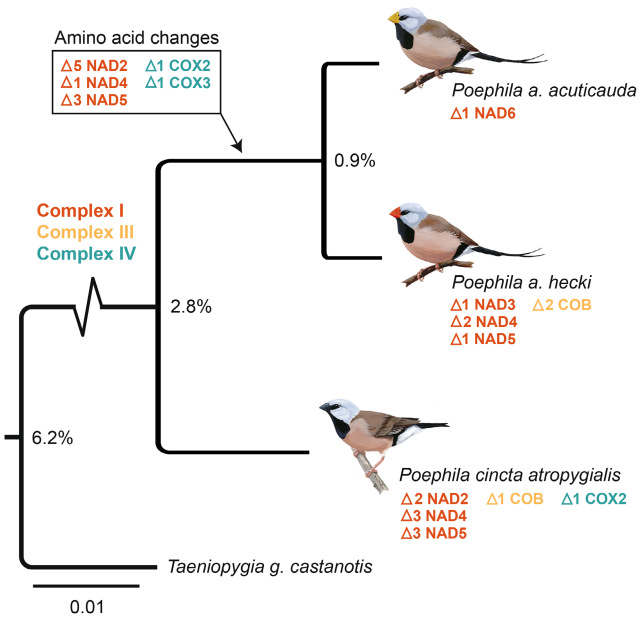

FIGURE 3 Evolutionary history of mtDNA protein-coding divergence between long-tailed finch subspecies. A maximum likelihood tree was generated based on an aligned concatenation of consensus sequences for all 13 protein-coding genes using W-IQ-TREE (Trifinopoulos et al., 2016) under the best-fit substitution model: TPM2u + F + I. The zebra finch (NCBI accession: DQ422742) and black-throated finch samples were used to assign all nucleotide substitutions and any associated amino acid changes to their branch of origin. Branch lengths are proportional to the number of substitutions. Divergence estimates at each node represent the total number of fixed differences between species in protein-coding genes divided by the total number of protein-coding bases (Table S3). The number of amino acid changes identified within each gene is colour-coded by ETS complex: red for complex I, yellow for complex III, and blue-green for complex IV.

TABLE 4 Model output comparing the measures of mitochondrial function among the six experimental groups.

	Interaction test		Variable of interest	Covariates			Variance explained				The significant differences between experimental groups				
	Cross*sex	Sex (if split model due to interaction)	Experimental group	Sex	Protein qty	Length of time					G5 < G6	G6 > G3	G2 < G6	G2 > G5	G5 < G4
Respiration measure	X^2 (DF) *p*-value		X^2 (DF) *p*-value	X^2 (DF) *p*-value	X^2 (DF) *p*-value	X^2 (DF) *p*-value	Variance	Marginal R^2	ICC pair ID	Conditional R^2	Showing *p*-values for $p < .1$				
OXP-I,II	**11.5 (5) .043**	Female	**12.73 (5) .026**	NA	2.59 (1) .11	**8.68 (1) .003**	197	.62	0.37	.99	*.064*			*.072*	
		Male	**13.87 (5) .016**	NA	**7.98 (1) .005**	**9.31 (1) .002**	240	.44	0.55	.99	**.042**		*.093*		
ETS-I,II	9.78 (5) .08	NA	**20.15 (5) .001**	2.3 (1) .13	**4.06 (1) .044**	**26.1 (1) < .001**	289	.53	0.46	.99	**<.001**	**.034**			
OXP-I	**11.97 (5) .035**	Female	**15.4 (5) .009**	NA	*3.29 (1) .07*	**25.2 (1) < .001**	206	.79	0.20	.99	**.029**			**.036**	
		Male	**14.9 (5) .010**	NA	**6.67 (1) .010**	**33.11 (1) < .001**	224	.63	0.36	.99	**.030**		*.052*		
ETS-II	7.1 (5) .2	NA	**19.6 (5) .002**	1.53 (1) .22	**5.04 (1) .02**	1.17 (1) .28	55	.39	0.58	.98	**.001**	*.065*			
CxIV	8.7 (5) .12	NA	**19.8 (5) .001**	1.5 (1) .22	**7.8 (1) .005**	2.14 (1) .14	302	.41	0.58	.99	**.001**				*.056*
LEAK-I,II	*9.6 (5) .09*	NA	**17.3 (5) .004**	2.4 (1) .12	**8.6 (1) .003**	0.3 (1) .58	1.4	.19	0.36	.55	**.003**				

Note: Group labels same as in Figure 4. Group 1 (G1); parental group *acuticauda*, Group 2 (G2): parental group *hecki*, Group 3 (G3): mitoconcordant backcross *acuticauda* mitotype, Group 4 (G4): mitoconcordant backcross *hecki* mitotype, Group 5 (G5): mitodiscordant backcross *acuticauda* mitotype, Group 6 (G6): mitodiscordant backcross *hecki* mitotype. ICC Pair ID—intra-class correlation coefficient value for Pair ID as a random effect.

Values in italics denote significance at $p < 0.1$ but not $p < 0.05$.

Values in bold represent a results of all genes combined.

TABLE 5 Model output comparing the physiology measures among the six experimental groups.

	Interaction test		Variable of interest	Covariates		Variance explained					Significant differences between experimental groups		
	Cross*sex		Experimental group	Sex	Embryo mass						G3 < G4	G1 < G4	G5 < G4
Measure	X^2 (DF) *p*-value	Sex (if split model due to interaction)	X^2 (DF) *p*-value	X^2 (DF) *p*-value	X^2 (DF) *p*-value	Variance	Marginal R^2	ICC pair ID	ICC plate	Conditional R^2	Showing *p*-values for $p < .1$		
Embryo Mass	8.6 (5) .13		7.3 (5) .20	0.01 (1) .92	NA	<0.001	<.001	<0.001	NA	<.001			
Embryo Survival	NA		4.1 (5) .53	NA	NA	0.09	.02	0.24	NA	.27			
Heart rate (proxy for whole-body metabolism)	**15.2 (5) .01**	Male	7.8 (5) .17	NA	**23.5 (1) < .01**	156	.41	0.59	NA	.99			
		Female	6.3 (5) .28	NA	**8.3 (1) .004**	78	.20	0.80		.99			
Oxidative DNA oxidative damage (log transformed)	8.3 (5) .14		8.6 (5) .12	*3.0 (1) .08*	NA	0.019	.006	0.012	0.008	.026			
mtDNA copy number (log transformed)	2.2 (5) .82		**20.9 (5) < .001**	0.17 (1) .69	NA	0.03	.01	0.02	0.00	.03	**.005**	*.093*	*.090*

Note: Group labels same as in Figure 4. Group 1 (G1); parental group *acuticauda*, Group 2 (G2): parental group *hecki*, Group 3 (G3): mitoconcordant backcross *acuticauda* mitotype, Group 4 (G4): mitoconcordant backcross *hecki* mitotype, Group 5 (G5): mitodiscordant backcross *acuticauda* mitotype, Group 6 (G6): mitodiscordant backcross *hecki* mitotype. ICC Pair ID—intra-class correlation coefficient value for Pair ID as a random effect.

Values in italics denote significance at $p < 0.1$ but not $p < 0.05$.

Values in bold represent a results of all genes combined.

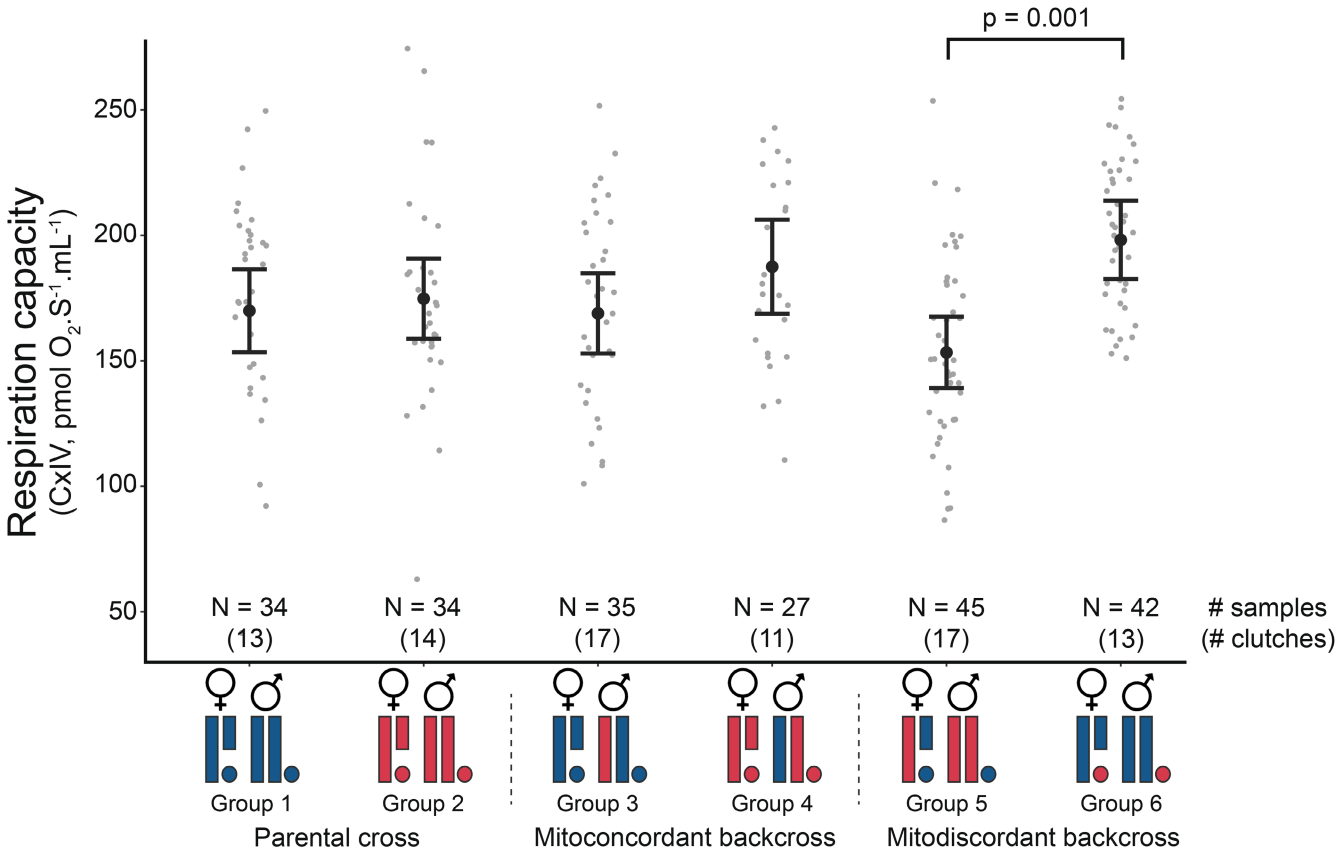

FIGURE 4 Mitochondrial and nuclear genomes between the long-tailed finch subspecies interact to impact mitochondrial respiration capacity. The respiration capacity of our experimental groups, with grey datapoints indicating raw data (corrected for amount of protein), and black mean and 95% CIs reflect model output (accounting for clutch ID, protein quantity, length of time in chamber, sex). Most measures of mitochondrial respiration capacity had this same pattern of differences among the groups (Table 5; Figure S2).

mitodiscordant backcross *hecki* mitotype was significantly higher than the mitoconcordant backcross *acuticauda* mitotype, and for OXP-I females the parental group *hecki* was significantly higher than the mitodiscordant backcross *acuticauda* mitotype group (Table 5).

We did not find a difference between groups in oxidative damage (Table 2, Figure S3D). We also found no evidence that this difference in aerobic respiration capacity between mitodiscordant backcross groups was driven by different quantities of mitochondria per cell, with the relative mtDNA copy number not significantly differing between the two mitodiscordant backcross groups, or between them and other groups (Table 2) and so likely not driving the aerobic respiration capacity results. We also found no difference between experimental groups in heart rate on day 12 of incubation immediately after being removed from the incubator and so no evidence that whole-body metabolism is impacted by hybrid cross (Table 2, Figure S3C).

4 | DISCUSSION

We found evidence that an interaction between the mitochondrial and nuclear genomes of long-tailed finch subspecies impacted aerobic respiration capacity in hybrids, despite the low level of mtDNA divergence between them (~1%). Our primary result suggests that while there is no difference in mitochondrial aerobic metabolism during the embryonic stage between each mitotype in the pure parental context, or in mitoconcordant backcross hybrids, mitodiscordant backcross hybrids with an *acuticauda* mitotype have reduced respiration capacity compared to those carrying a *hecki* mitotype. Respiration capacity reflects the upper limit of mitochondrial aerobic respiration. Therefore, the reduced aerobic capacity observed for mitodiscordant backcross individuals with an *acuticauda* mitotype might be expected to be detrimental, particularly for energetically demanding tissues, life stages, and environments. The effect of mitonuclear interactions on aerobic respiration we have identified has important implications for both mtDNA introgression and reproductive isolation in the long-tailed finch system. There are high levels of admixture in the long-tailed finch hybrid zone (68% of individuals have some degree of mitonuclear mismatch, 243 of 357 samples (Lopez et al., 2021)), and so selection can act on each mitotype in several distinct nuclear contexts, akin to those generated through our experimental approach. In the regime of widespread admixture that exists within the hybrid zone, selection against the *acuticauda* mitotype in mitodiscordant hybrids might result in the *hecki* mitotype increasing in frequency and introgressing westwards

as a result. This is indeed what is observed in the wild long-tailed finch hybrid zone. Mitodiscordant hybrids with an *acuticauda* mitotype are rare compared to those with a *hecki* mitotype (83% of mitodiscordant hybrids carry a *hecki* mitotype, 57 of 69 samples (Lopez et al., 2021)), and the centre of the mitochondrial cline is displaced 55 km west of the nuclear cline centre (Figure 1b, c). This suggests that the physiological effects observed in this experiment may be a good proxy for the selection that is occurring in the wild. We discuss the implications and limitations of our results further below.

We did not find strong evidence that mitonuclear incompatibilities reduce hybrid embryo fitness compared to parental individuals. There were few differences between our mitodiscordant backcross groups and either pure parental individuals or mitoconcordant backcross groups (Table 5; Figure 4 and Figure S2). A conservative interpretation would suggest that incompatibility between the mitochondrial and nuclear genomes of these subspecies is not a key component of reproductive isolation in the long-tailed finch system, which might instead be linked to other incompatibilities such as those involving chromosomal inversions (Hooper et al., 2019). Our lack of difference between parental and mitodiscordant backcross groups is in stark contrast to results from comparable experiments using deeply diverged lineages crossed in the lab (e.g. with mitochondrial divergence >10%), where mitodiscordant backcrossed individuals had dramatically impacted mitochondrial function, survival, or fecundity (Barreto et al., 2018; Barreto & Burton, 2013; Ellison et al., 2008; Ellison & Burton, 2008). There are, however, some lines of evidence suggestive of nascent mitonuclear incompatibility in this study, and we may simply not have had enough statistical power to detect weak effects. For a few respiration measures, there were significant—or borderline significant—differences between mitodiscordant and mitoconcordant backcross groups; for ETS-I,II (Figure 4) and ETS-II mitodiscordant backcrosses with a *hecki* mitotype had higher respiration capacity than did mitoconcordant backcrosses with an *acuticauda* mitotype, and for CxIV mitodiscordant backcrosses with an *acuticauda* mitotype had borderline significantly lower respiration capacity than *hecki* mitoconcordant backcrosses (Table 5; Figure S2). Mitonuclear dysfunction may only become apparent in specific tissue types with high baseline energy consumption (e.g. cardiac or nervous system tissue) or under stressful conditions with heightened energetic demands (e.g. during reproduction or thermal stress). Thus, our observations do not preclude a role for mitonuclear incompatibilities as a reproductive isolating barrier at this early stage of population divergence.

While not statistically significant, the mean respiration values of both mitodiscordant backcross groups deviated from the parental groups (Figure 4). To the extent that aerobic metabolism efficiency is shaped by selection (Baris et al., 2016; Gangloff et al., 2020; Rozas et al., 2017), deviations below—or above—species or life-stage specific optima could prove deleterious. These costs are likely to be context dependent and are not necessarily expected to be symmetrical in their effects (Monzel et al., 2023). As we discussed above, the reduced respiration capacity observed in *acuticauda* carrying mitodiscordant hybrids is paired with their rarity in the wild hybrid zone. The increased respiration capacity observed in *hecki* carrying mitodiscordant hybrids is associated in turn with introgression of the *hecki* mitotype across the hybrid zone but not beyond it into a pure *acuticauda* nuclear genetic background. Will the *hecki* mitotype continue to introgress westwards? Perhaps not, if indeed the aerobic metabolism of mitodiscordant individuals with *hecki* mitotype is above the species or life-stage specific optima. Climate-mediated selection appears to explain the geography of mitochondrial variation in many Australian songbird species (Morales et al., 2018; Nagarajan-Radha et al., 2020). Intriguingly, the centre of mitochondrial admixture between long-tailed finch subspecies is located along the edge of the Kimberley Plateau (Meiklejohn et al., 2013), a unique bioregion in Western Australia with a distinct climate, climatic history, geology, landform, and vegetation compared to the rest of the species' range (Pepper & Keogh, 2014; Shelley et al., 2019). Further study is required to evaluate whether the increased respiration capacity of *hecki* carrying mitodiscordant hybrids might be costly within the climatic regime of the Kimberley Plateau and limit further introgression.

We were interested in distinguishing what mitonuclear components were likely interacting to impact mitochondrial aerobic respiration. We wanted to know whether the observed differences in aerobic respiration between mitodiscordant backcross groups were the result of specific protein–protein interactions in complexes I and III or if instead they were due to interactions involving mtDNA-encoded tRNA or rRNA. The difference between the two mitodiscordant backcross groups was consistent across all measures, which included the CxIV respiration measure that is not dependent on other complexes, and there are no fixed differences in CxIV amino acids between subspecies. This suggests that the causal mitonuclear interaction may not be between proteins encoded by the two genomes but may instead be between either mtDNA-encoded tRNA and nuDNA-encoded aminoacyl tRNA synthetases, or between mtDNA-encoded rRNA and nuDNA-encoded ribosomal proteins. These interactions would impact the translation of mtDNA and therefore the production of all mtDNA-encoded ETS complexes (CxI, III, IV, and V).

There was also a significant sex difference in the *hecki* subspecies for two measures (OXP-I,II and OXP-I), whereby females had higher respiration capacity than males (Table 5). As a result, *hecki* females had higher respiration capacity than mitodiscordant hybrids of both sexes carrying an *acuticauda* mitotype, and *hecki* males had lower respiration capacity than mitodiscordant hybrids of both sexes carrying a *hecki* mitotype. It is unclear to us why there is a sex difference in respiration capacity for *hecki* individuals but not *acuticauda* or backcrossed individuals. This may just be a false positive, as we have run many statistical tests in this study, but it could be biological; sex differences in mitochondrial function have been observed in the literature, although there is no apparent consistent difference (Junker et al., 2022). Furthermore, as embryos we would not expect dramatic sex differences in metabolism, except perhaps for the gonads. 'Mother's curse' is a phenomenon that can result in a sex effect due to mitonuclear interactions (Carnegie et al., 2021;

Dowling & Adrian, 2019; Nagarajan-Radha et al., 2020), but it predicts that detrimental impacts of mtDNA on males and resulting sex differences are exposed with heterospecific nuDNA but not homospecific nuDNA (due to nuDNA coevolution to rescue function), whereas in the present study we found the opposite; that seemingly detrimental impacts of mtDNA only occurs in homo(sub)specific nuDNA context.

We did not find evidence that the observed effects on cellular aerobic respiration capacity between mitodiscordant backcross groups affected our proxies for whole-organism metabolic rate or the level of oxidative damage. The inter-lineage mitonuclear interactions may therefore be impacting fitness through other pathways or under specific circumstances, for example, in energetically demanding tissues and life stages. Given the experimental context, it would also be valuable to confirm the whole-body result with more direct measures of metabolism (e.g. open-flow respirometry (Cooper et al., 2020)). This is because other differences between experimental groups may undermine how well heart rate reflects differences in whole-body metabolism, for example, at low incubation temperature, Japanese quail heart rate decreases (Stier et al., 2020) but heart volume increases to compensate (A. Stier, unpublished data).

Purifying selection appears to be the dominant force in mtDNA evolution in *Poephila* (the mitochondrial genome-wide dN/dS ratio is well below 1 at 0.0168). The observed amino acid differences between long-tailed finch subspecies are thus notable, with all six *hecki*-derived amino acid changes in genes within complexes I (four AAs) and III (two AAs) suggesting some degree of inter-molecular epistasis might exist between these substitutions. Moreover, in one of the genes with multiple non-synonymous substitutions (COB), amino acid changes were located <15 codon positions apart, a possible signature of intra-molecular epistasis (Callahan et al., 2011; Storz, 2018). Taken together this may constitute evidence of adaptive evolution within *hecki*, as mitochondria can contribute to local adaptation (e.g. to differences in climate) (Lajbner et al., 2018; Lamb et al., 2018; Lasne et al., 2019), but to confirm this requires further investigation.

In conclusion, we here demonstrate that functional consequences of interactions between mtDNA and nuDNA are possible even at a low level of divergence (~1% mtDNA), and the resulting impact on fitness between the two groups with mitonuclear mismatch in this system may be strong enough to result in asymmetrical mitochondrial introgression across a hybrid zone. Such mitonuclear interactions may be widespread, as most avian lineages with stable hybrid zones have equal or greater divergence. Researchers considering cases of mitonuclear discordance (or cytonuclear discordance more generally) should consider that functional consequences of mitonuclear interactions may be at play (Nikelski et al., 2023; Wang et al., 2021). We note that our experimental design tested for evidence of mitonuclear interactions manifesting during embryonic development, and that additional work examining variation in aerobic metabolism at post-natal stages under the physiologically demanding conditions these birds experience in the wild may reveal further differences between the different crosses. Identifying the specific genes involved in mitonuclear interactions in the long-tailed finch would also be a valuable direction for future research, as this will facilitate testing the molecular pathways involved in mitonuclear interactions and the evolutionary processes that led to them (e.g. rapid evolution) (Baris et al., 2017; Barreto et al., 2018; Healy & Burton, 2022a, 2022b; Moran et al., 2022; Nguyen et al., 2022). This sensitivity of mitochondrial function to genetic variation, their centrality to organismal function (generating 90% of cellular energy in animals (Harris & Das, 1991)), and the broad range of taxa that rely on mitochondria for energy production support suggestions that mitonuclear interactions may be a powerful force acting on hybridizing animals (Hill, 2016; Hill et al., 2019; Pereira et al., 2021; Wolff et al., 2014).

AUTHOR CONTRIBUTIONS

Conceptualization, C.S.M., S.C.G.; Methodology, C.S.M., D.M.H., A.S., S.C.G; Investigation, C.S.M.; Data analysis and interpretation, C.S.M., D.M.H., A.S.; Resources, S.C.G.; Writing—Original Draft, C.S.M.; Writing—Review & Editing, C.S.M, D.M.H., A.S., S.C.G.; Visualization, C.S.M., D.M.H.; Supervision, S.C.G.; Funding Acquisition, C.S.M., D.M.H., S.C.G.

ACKNOWLEDGEMENTS

The authors would like to thank Riccardo Ton and Hector Pacheco Fuentes for providing assistance in setting up the Oroboros O_2k, and Macquarie Animal Research Services (M.A.R.S.) staff for providing daily bird husbandry. Open access publishing facilitated by Macquarie University, as part of the Wiley - Macquarie University agreement via the Council of Australian University Librarians.

FUNDING INFORMATION

This work was supported by an Australian Research Council (ARC) Discovery Project to SCG and DMH (DP180101783), and a Holsworth Wildlife Research Endowment from Equity Trustees Charitable Foundation and the Ecological Society of Australia and a Macquarie University Research Excellence Scholarship to CSM. AS was supported by a 'Turku Collegium for Science and Medicine' Fellowship and a Marie Sklodowska-Curie Postdoctoral Fellowship (#894963). Gerstner Scholars Fellowship and the Gerstner Family Foundation, and the Richard Gilder Graduate School at the American Museum of Natural History provided support to DMH.

CONFLICT OF INTEREST STATEMENT

The authors declare no competing interests.

OPEN RESEARCH BADGES

This article has earned an Open Data badge for making publicly available the digitally-shareable data necessary to reproduce the reported results. The data is available at [https://doi.org/10.5061/dryad.m37pvmd9v].

DATA AVAILABILITY STATEMENT

Data from the respiration capacity, oxidative damage, heart rate and mitochondrial copy number, the R scripts for statistical analyses are available on Dryad (doi:10.5061/dryad.m37pvmd9v). Mitochondrial genome assemblies are available on GenBank (PP372643–PP372678). The WGS data used to assemble mitogenomes are available via SRA under the BioProject accession PRJNA1101033.

ETHICS STATEMENT

This experiment was approved by the Macquarie University Animal Ethics Committee (reference number: 2020/021), and all experiments conform to the relevant regulatory standards.

ORCID

Callum S. McDiarmid https://orcid.org/0000-0003-2938-7176
Daniel M. Hooper https://orcid.org/0000-0002-4198-4320
Antoine Stier https://orcid.org/0000-0002-5445-5524
Simon C. Griffith https://orcid.org/0000-0001-7612-4999

REFERENCES

Allio, R., Donega, S., Galtier, N., & Nabholz, B. (2017). Large variation in the ratio of mitochondrial to nuclear mutation rate across animals: Implications for genetic diversity and the use of mitochondrial DNA as a molecular marker. *Molecular Biology and Evolution*, *34*, 2762–2772. https://doi.org/10.1093/molbev/msx197

Arnqvist, G., Dowling, D. K., Eady, P., Gay, L., Tregenza, T., Tuda, M., & Hosken, D. J. (2010). Genetic architecture of metabolic rate: Environment specific epistasis between mitochondrial and nuclear genes in an insect. *Evolution*, *64*, 3354–3363. https://doi.org/10.1111/j.1558-5646.2010.01135.x

Baris, T. Z., Blier, P. U., Pichaud, N., Crawford, D. L., & Oleksiak, M. F. (2016). Gene by environmental interactions affecting oxidative phosphorylation and thermal sensitivity. *The American Journal of Physiology-Regulatory, Integrative and Comparative Physiology*, *311*, R157–R165. https://doi.org/10.1152/ajpregu.00008.2016

Baris, T. Z., Wagner, D. N., Dayan, D. I., Du, X., Blier, P. U., Pichaud, N., Oleksiak, M. F., & Crawford, D. L. (2017). Evolved genetic and phenotypic differences due to mitochondrial-nuclear interactions. *PLoS Genetics*, *13*, e1006517. https://doi.org/10.1371/journal.pgen.1006517

Barreto, F. S., & Burton, R. S. (2013). Elevated oxidative damage is correlated with reduced fitness in interpopulation hybrids of a marine copepod. *Proceedings of the Royal Society B*, *280*, 20131521. https://doi.org/10.1098/rspb.2013.1521

Barreto, F. S., Watson, E. T., Lima, T. G., Willett, C. S., Edmands, S., Li, W., & Burton, R. S. (2018). Genomic signatures of mitonuclear coevolution across populations of Tigriopus californicus. *Nature Ecology & Evolution*, *2*, 1250–1257. https://doi.org/10.1038/s41559-018-0588-1

Bar-Yaacov, D., Blumberg, A., & Mishmar, D. (2012). Mitochondrial-nuclear co-evolution and its effects on OXPHOS activity and regulation. *Biochimica et Biophysica Acta (BBA)—Gene Regulatory Mechanisms*, *1819*, 1107–1111. https://doi.org/10.1016/j.bbagrm.2011.10.008

Bar-Yaacov, D., Hadjivasiliou, Z., Levin, L., Barshad, G., Zarivach, R., Bouskila, A., & Mishmar, D. (2015). Mitochondrial involvement in vertebrate speciation? The case of Mito-nuclear genetic divergence in chameleons. *Genome Biology and Evolution*, *7*, 3322–3336. https://doi.org/10.1093/gbe/evv226

Bates, D., Mächler, M., Bolker, B., & Walker, S. (2015). Fitting linear mixed-effects models using lme4. *Journal of Statistical Software*, *67*, 1–47\8. https://doi.org/10.18637/jss.v067.i01

Birben, E., Sahiner, U. M., Sackesen, C., Erzurum, S., & Kalayci, O. (2012). Oxidative stress and antioxidant defense. *World Allergy Organization Journal*, *5*, 9–19. https://doi.org/10.1097/wox.0b013e3182439613

Bonnet, T., Leblois, R., Rousset, F., & Crochet, P.-A. (2017). A reassessment of explanations for discordant introgressions of mitochondrial and nuclear genomes. *Evolution*, *71*, 2140–2158. https://doi.org/10.1111/evo.13296

Brazill-Boast, J., van Rooij, E. P., Pryke, S. R., & Griffith, S. C. (2011). Interference from long-tailed finches constrains reproduction in the endangered Gouldian finch. *The Journal of Animal Ecology*, *80*, 39–48.

Burton, R. S., Pereira, R. J., & Barreto, F. S. (2013). Cytonuclear genomic interactions and hybrid breakdown. *Annual Review of Ecology, Evolution, and Systematics*, *44*, 281–302. https://doi.org/10.1146/annurev-ecolsys-110512-135758

Callahan, B., Neher, R. A., Bachtrog, D., Andolfatto, P., & Shraiman, B. I. (2011). Correlated evolution of nearby residues in Drosophilid proteins. *PLoS Genetics*, *7*, e1001315. https://doi.org/10.1371/journal.pgen.1001315

Carnegie, L., Reuter, M., Fowler, K., Lane, N., & Camus, M. F. (2021). Mother's curse is pervasive across a large mitonuclear drosophila panel. *Evolution Letters*, *5*, 230–239. https://doi.org/10.1002/evl3.221

Chou, J., & Leu, J. (2010). Speciation through cytonuclear incompatibility: Insights from yeast and implications for higher eukaryotes. *BioEssays*, *32*, 401–411. https://doi.org/10.1002/bies.200900162

Cooper, C. E., Hurley, L. L., & Griffith, S. C. (2020). Effect of acute exposure to high ambient temperature on the thermal, metabolic and hygric physiology of a small desert bird. *Comparative Biochemistry and Physiology. Part A, Molecular & Integrative Physiology*, *244*, 110684. https://doi.org/10.1016/j.cbpa.2020.110684

Coyne, J. A., & Orr, H. A. (2004). *Speciation*. Sinauer Associates.

Donath, A., Jühling, F., Al-Arab, M., Bernhart, S. H., Reinhardt, F., Stadler, P. F., Middendorf, M., & Bernt, M. (2019). Improved annotation of protein-coding genes boundaries in metazoan mitochondrial genomes. *Nucleic Acids Research*, *47*, 10543–10552. https://doi.org/10.1093/nar/gkz833

Dowling, D. K., & Adrian, R. E. (2019). Challenges and prospects for testing the Mother's curse hypothesis. *Integrative and Comparative Biology*, *59*, 875–889. https://doi.org/10.1093/icb/icz110

Ellison, C. K., & Burton, R. S. (2008). Interpopulation hybrid breakdown maps to the mitochondrial genome. *Evolution*, *62*, 631–638. https://doi.org/10.1111/j.1558-5646.2007.00305.x

Ellison, C. K., Niehuis, O., & Gadau, J. (2008). Hybrid breakdown and mitochondrial dysfunction in hybrids of Nasonia parasitoid wasps. *Journal of Evolutionary Biology*, *21*, 1844–1851. https://doi.org/10.1111/j.1420-9101.2008.01608.x

Gangloff, E. J., Schwartz, T. S., Klabacka, R., Huebschman, N., Liu, A.-Y., & Bronikowski, A. M. (2020). Mitochondria as central characters in a complex narrative: Linking genomics, energetics, pace-of-life, and aging in natural populations of garter snakes. *Experimental Gerontology*, *137*, 110967. https://doi.org/10.1016/j.exger.2020.110967

Gao, F., Chen, C., Arab, D. A., Du, Z., He, Y., & Ho, S. Y. W. (2019). EasyCodeML: A visual tool for analysis of selection using CodeML. *Ecology and Evolution*, *9*, 3891–3898. https://doi.org/10.1002/ece3.5015

Hahn, A., & Zuryn, S. (2019). The cellular mitochondrial genome landscape in disease. *Trends in Cell Biology*, *29*, 227–240. https://doi.org/10.1016/j.tcb.2018.11.004

Harris, D. A., & Das, A. M. (1991). Control of mitochondrial ATP synthesis in the heart. *The Biochemical Journal*, *280*, 561–573. https://doi.org/10.1042/bj2800561

Hartig, F. (2021). Residual Diagnostics for Hierarchical (Multi-Level/Mixed) Regression Models [R package DHARMa version 0.4.4].

Healy, T. M., & Burton, R. S. (2022a). Differential gene expression and mitonuclear incompatibilities in fast- and slow-developing inter-population Tigriopus californicus hybrids. Biorxiv, 2022.09.09.507197 https://doi.org/10.1101/2022.09.09.507197

Healy, T. M., & Burton, R. S. (2022b). Genetic incompatibilities in reciprocal hybrids between populations of *Tigriopus californicus* with low to moderate mitochondrial sequence divergence. Biorxiv, 2022.09.19.508600. https://doi.org/10.1101/2022.09.19.508600

Hill, G. E. (2016). Mitonuclear coevolution as the genesis of speciation and the mitochondrial DNA barcode gap. *Ecology and Evolution*, *6*, 5831–5842. https://doi.org/10.1002/ece3.2338

Hill, G. E. (2017). The mitonuclear compatibility species concept. *The Auk*, *134*, 393–409. https://doi.org/10.1642/auk-16-201.1

Hill, G. E. (2019a). *Mitonuclear ecology*. Oxford University Press.

Hill, G. E. (2019b). Reconciling the Mitonuclear compatibility species concept with rampant mitochondrial introgression. *Integrative and Comparative Biology*, *59*, 912–924. https://doi.org/10.1093/icb/icz019

Hill, G. E. (2020). Mitonuclear compensatory coevolution. *Trends in Genetics*, *36*, 403–414. https://doi.org/10.1016/j.tig.2020.03.002

Hill, G. E., Havird, J. C., Sloan, D. B., Burton, R. S., Greening, C., & Dowling, D. K. (2019). Assessing the fitness consequences of mitonuclear interactions in natural populations. *Biological Reviews*, *94*, 1089–1104. https://doi.org/10.1111/brv.12493

Hooper, D. M., Griffith, S. C., & Price, T. D. (2019). Sex chromosome inversions enforce reproductive isolation across an avian hybrid zone. *Molecular Ecology*, *28*, 1246–1262. https://doi.org/10.1111/mec.14874

Junker, A., Wang, J., Gouspillou, G., Ehinger, J. K., Elmér, E., Sjövall, F., Fisher-Wellman, K. H., Neufer, P. D., Molina, A. J. A., Ferrucci, L., & Picard, M. (2022). Human studies of mitochondrial biology demonstrate an overall lack of binary sex differences: A multivariate meta-analysis. *The FASEB Journal*, *36*, e22146. https://doi.org/10.1096/fj.202101628r

Katoh, K., Rozewicki, J., & Yamada, K. D. (2017). MAFFT online service: Multiple sequence alignment, interactive sequence choice and visualization. *Briefings in Bioinformatics*, *20*, 1160–1166. https://doi.org/10.1093/bib/bbx108

Koch, R. E., Buchanan, K. L., Casagrande, S., Crino, O., Dowling, D. K., Hill, G. E., Hood, W. R., McKenzie, M., Mariette, M. M., Noble, D. W. A., Pavlova, A., Seebacher, F., Sunnucks, P., Udino, E., White, C. R., Salin, K., & Stier, A. (2021). Integrating mitochondrial aerobic metabolism into ecology and evolution. *Trends in Ecology & Evolution*, *36*, 321–332. https://doi.org/10.1016/j.tree.2020.12.006

Kuznetsova, A., Brockhoff, P., & Christensen, R. (2017). lmerTest package: Tests in linear mixed effects models. *Journal of Statistical Software*, *82*, 1–26. https://doi.org/10.18637/jss.v082.i13

Lajbner, Z., Pnini, R., Camus, M. F., Miller, J., & Dowling, D. K. (2018). Experimental evidence that thermal selection shapes mitochondrial genome evolution. *Scientific Reports-UK*, *8*, 9500. https://doi.org/10.1038/s41598-018-27805-3

Lamb, A. M., Gan, H. M., Greening, C., Joseph, L., Lee, Y. P., Morán-Ordóñez, A., Sunnucks, P., & Pavlova, A. (2018). Climate-driven mitochondrial selection: A test in Australian songbirds. *Molecular Ecology*, *27*, 898–918. https://doi.org/10.1111/mec.14488

Lasne, C., Heerwaarden, B., Sgrò, C. M., & Connallon, T. (2019). Quantifying the relative contributions of the X chromosome, autosomes, and mitochondrial genome to local adaptation*. *Evolution*, *73*, 262–277. https://doi.org/10.1111/evo.13647

Lee, H.-Y., Chou, J.-Y., Cheong, L., Chang, N.-H., Yang, S.-Y., & Leu, J.-Y. (2008). Incompatibility of nuclear and mitochondrial genomes causes hybrid sterility between two yeast species. *Cell*, *135*, 1065–1073. https://doi.org/10.1016/j.cell.2008.10.047

Lee, J. C.-I., Tsai, L. C., Hwa, P. Y., Chan, C. L., Huang, A., Chin, S. C., Wang, L. C., Lin, J. T., Linacre, A., & Hsieh, H. M. (2010). A novel strategy for avian species and gender identification using the CHD gene. *Molecular and Cellular Probes*, *24*, 27–31. https://doi.org/10.1016/j.mcp.2009.08.003

Lenth, R. (2020). emmeans: Estimated Maringal Means, aka Least-Squares Means. R package.

Li, H. (2011). A statistical framework for SNP calling, mutation discovery, association mapping and population genetical parameter estimation from sequencing data. *Bioinformatics*, *27*, 2987–2993. https://doi.org/10.1093/bioinformatics/btr509

Lopez, K. A., McDiarmid, C. S., Griffith, S. C., Lovette, I. J., & Hooper, D. M. (2021). Evaluating evidence of mitonuclear incompatibilities with the sex chromosomes in an avian hybrid zone. *Evolution*, *75*, 1395–1414. https://doi.org/10.1111/evo.14243

Ma, H., Marti Gutierrez, N., Morey, R., van Dyken, C., Kang, E., Hayama, T., Lee, Y., Li, Y., Tippner-Hedges, R., Wolf, D. P., Laurent, L. C., & Mitalipov, S. (2016). Incompatibility between nuclear and mitochondrial genomes contributes to an interspecies reproductive barrier. *Cell Metabolism*, *24*, 283–294. https://doi.org/10.1016/j.cmet.2016.06.012

Marasco, V., Stier, A., Boner, W., Griffiths, K., Heidinger, B., & Monaghan, P. (2017). Environmental conditions can modulate the links among oxidative stress, age, and longevity. *Mechanisms of Ageing and Development*, *164*, 100–107. https://doi.org/10.1016/j.mad.2017.04.012

Markkanen, E. (2017). Not breathing is not an option: How to deal with oxidative DNA damage. *DNA Repair*, *59*, 82–105. https://doi.org/10.1016/j.dnarep.2017.09.007

Martindale, J. L., & Holbrook, N. J. (2002). Cellular response to oxidative stress: Signaling for suicide and survival*. *Journal of Cellular Physiology*, *192*, 1–15. https://doi.org/10.1002/jcp.10119

Meiklejohn, C. D., Holmbeck, M. A., Siddiq, M. A., Abt, D. N., Rand, D. M., & Montooth, K. L. (2013). An incompatibility between a mitochondrial tRNA and its nuclear-encoded tRNA synthetase compromises development and fitness in drosophila. *PLoS Genetics*, *9*, e1003238. https://doi.org/10.1371/journal.pgen.1003238

Montooth, K. L., Meiklejohn, C. D., Abt, D. N., & Rand, D. M. (2010). Mitochondrial-nuclear epistasis affects fitness within species but does not contribute to fixed incompatibilities between species of drosophila. *Evolution*, *64*, 3364–3379. https://doi.org/10.1111/j.1558-5646.2010.01077.x

Monzel, A. S., Enríquez, J. A., & Picard, M. (2023). Multifaceted mitochondria: Moving mitochondrial science beyond function and dysfunction. *Nature Metabolism*, *5*, 546–562. https://doi.org/10.1038/s42255-023-00783-1

Morales, H. E., Pavlova, A., Amos, N., Major, R., Kilian, A., Greening, C., & Sunnucks, P. (2018). Concordant divergence of mitogenomes and a mitonuclear gene cluster in bird lineages inhabiting different climates. *Nature Ecology & Evolution*, *2*, 1258–1267. https://doi.org/10.1038/s41559-018-0606-3

Moran, B., Payne, C. Y., Powell, D. L., Iverson, E. N. K., Donny, A. E., Banerjee, S. M., Langdon, Q. K., Gunn, T. R., Rodriguez-Soto, R. A., Madero, A., Baczenas, J. J., Kleczko, K. M., Liu, F., Matney, R., et al. (2022). A lethal genetic incompatibility between naturally hybridizing species in mitochondrial complex I. 1–45.

Mower, J. P., Touzet, P., Gummow, J. S., Delph, L. F., & Palmer, J. D. (2007). Extensive variation in synonymous substitution rates in mitochondrial genes of seed plants. *BMC Evolutionary Biology*, *7*, 135. https://doi.org/10.1186/1471-2148-7-135

Nabholz, B., Glémin, S., & Galtier, N. (2008). Strong variations of mitochondrial mutation rate across mammals—The longevity hypothesis. *Molecular Biology and Evolution*, *25*, 120–130. https://doi.org/10.1093/molbev/msm248

Nabholz, B., Glémin, S., & Galtier, N. (2009). The erratic mitochondrial clock: Variations of mutation rate, not population size, affect mtDNA diversity across birds and mammals. *BMC Evolutionary Biology*, *9*, 54. https://doi.org/10.1186/1471-2148-9-54

Nagarajan-Radha, V., Aitkenhead, I., Clancy, D. J., Chown, S. L., & Dowling, D. K. (2020). Sex-specific effects of mitochondrial haplotype on metabolic rate in Drosophila melanogaster support predictions of the Mother's curse hypothesis. *Philosophical Transactions of the Royal Society B*, *375*, 20190178. https://doi.org/10.1098/rstb.2019.0178

Nguyen, T. H. M., Tinz-Burdick, A., Lenhardt, M., Geertz, M., Ramirez, F., Schwartz, M., Toledano, M., Bonney, B., Gaebler, B., Liu, W., Wolters, J. F., Chiu, K., Fiumera, A. C., & Fiumera, H. L. (2022). Mapping mitonuclear epistasis using a novel recombinant yeast population. Biorxiv, 2022.08.31.505974. https://doi.org/10.1101/2022.08.31.505974

Nikelski, E., Rubtsov, A. S., & Irwin, D. (2023). High heterogeneity in genomic differentiation between phenotypically divergent songbirds: A test of mitonuclear co-introgression. *Heredity*, *130*(1), 1–13. https://doi.org/10.1038/s41437-022-00580-8

Pepper, M., & Keogh, J. S. (2014). Biogeography of the Kimberley, Western Australia: A review of landscape evolution and biotic response in an ancient refugium. *Journal of Biogeography*, *41*, 1443–1455. https://doi.org/10.1111/jbi.12324

Pereira, R. J., Lima, T. G., Pierce-Ward, N. T., Chao, L., & Burton, R. S. (2021). Recovery from hybrid breakdown reveals a complex genetic architecture of mitonuclear incompatibilities. *Molecular Ecology*, *30*, 6403–6416. https://doi.org/10.1111/mec.15985

R Core Team. (2020). *R: A language and environment for statistical computing*. R Foundation for Statistical Computing.

Rowe, M., Griffith, S. C., Hofgaard, A., & Lifjeld, J. T. (2015). Subspecific variation in sperm morphology and performance in the Long-tailed Finch (*Poephila acuticauda*). *Avian Research*, *6*, 1–10. https://doi.org/10.1186/s40657-015-0032-z

Rozas, J., Ferrer-Mata, A., Sánchez-DelBarrio, J. C., Guirao-Rico, S., Librado, P., Ramos-Onsins, S. E., & Sánchez-Gracia, A. (2017). DnaSP 6: DNA sequence polymorphism analysis of large data sets. *Molecular Biology and Evolution*, *34*, 3299–3302. https://doi.org/10.1093/molbev/msx248

RStudio Team. (2020). *RStudio: Integrated development for R*. RStudio, PBC. http://www.rstudio.com/

Sheldon, E. L., McCowan, L. S. C., McDiarmid, C. S., & Griffith, S. C. (2018). Measuring the embryonic heart rate of wild birds: An opportunity to take the pulse on early development. *The Auk*, *135*, 71–82. https://doi.org/10.1642/auk-17-111.1

Shelley, J. J., Unmack, P. J., Dempster, T., Feuvre, M. C. L., & Swearer, S. E. (2019). The Kimberley, north-Western Australia, as a cradle of evolution and endemic biodiversity: An example using grunters (Terapontidae). *Journal of Biogeography*, *46*, 2420–2432. https://doi.org/10.1111/jbi.13682

Singhal, S., Leffler, E. M., Sannareddy, K., Turner, I., Venn, O., Hooper, D. M., Strand, A. I., Li, Q., Raney, B., Balakrishnan, C. N., Griffith, S. C., McVean, G., & Przeworski, M. (2015). Stable recombination hotspots in birds. *Science*, *350*(6263), 928–932.

Sloan, D. B., Havird, J. C., & Sharbrough, J. (2017). The on-again, off-again relationship between mitochondrial genomes and species boundaries. *Molecular Ecology*, *26*, 2212–2236. https://doi.org/10.1111/mec.13959

Sorenson, M. D., & Quinn, T. W. (1998). Numts: A challenge for avian systematics and population biology. *Auk*, *115*, 214–221. https://doi.org/10.2307/4089130

Stewart, J. B., & Chinnery, P. F. (2015). The dynamics of mitochondrial DNA heteroplasmy: Implications for human health and disease. *Nature Reviews. Genetics*, *16*, 530–542. https://doi.org/10.1038/nrg3966

Stier, A., Metcalfe, N. B., & Monaghan, P. (2020). Pace and stability of embryonic development affect telomere dynamics: An experimental study in a precocial bird model. *Proceedings of the Royal Society B*, *287*, 20201378. https://doi.org/10.1098/rspb.2020.1378

Stier, A., Monaghan, P., & Metcalfe, N. B. (2022). Experimental demonstration of prenatal programming of mitochondrial aerobic metabolism lasting until adulthood. *Proceedings of the Royal Society B*, *289*, 20212679. https://doi.org/10.1098/rspb.2021.2679

Stier, A., Romestaing, C., Schull, Q., Lefol, E., Robin, J., Roussel, D., & Bize, P. (2017). How to measure mitochondrial function in birds using red blood cells: A case study in the king penguin and perspectives in ecology and evolution. *Methods in Ecology and Evolution*, *8*, 1172–1182. https://doi.org/10.1111/2041-210x.12724

Stier, A., Schull, Q., Bize, P., Lefol, E., Haussmann, M., Roussel, D., Robin, J.-P., & Viblanc, V. A. (2019). Oxidative stress and mitochondrial responses to stress exposure suggest that king penguins are naturally equipped to resist stress. *Scientific Reports-Uk*, *9*, 8545. https://doi.org/10.1038/s41598-019-44990-x

Storz, J. F. (2018). Compensatory mutations and epistasis for protein function. *Current Opinion in Structural Biology*, *50*, 18–25. https://doi.org/10.1016/j.sbi.2017.10.009

Toews, D. P. L., & Brelsford, A. (2012). The biogeography of mitochondrial and nuclear discordance in animals. *Molecular Ecology*, *21*, 3907–3930. https://doi.org/10.1111/j.1365-294x.2012.05664.x

Toews, D. P. L., Mandic, M., Richards, J. G., & Irwin, D. E. (2014). Migration, mitochondria, and the yellow-rumped warbler. *Evolution*, *68*(1), 241–255. https://doi.org/10.5061/dryad.99db2

Ton, R., Stier, A., Cooper, C. E., & Griffith, S. C. (2021). Effects of heat waves during post-natal development on mitochondrial and whole body physiology: An experimental study in zebra finches. *Frontiers in Physiology*, *12*, 661670. https://doi.org/10.3389/fphys.2021.661670

Trifinopoulos, J., Nguyen, L.-T., von Haeseler, A., & Minh, B. Q. (2016). W-IQ-TREE: A fast online phylogenetic tool for maximum likelihood analysis. *Nucleic Acids Research*, *44*, W232–W235. https://doi.org/10.1093/nar/gkw256

Valavanidis, A., Vlachogianni, T., & Fiotakis, C. (2009). 8-hydroxy-2′-deoxyguanosine (8-OHdG): A critical biomarker of oxidative stress and carcinogenesis. *Journal of Environmental Science and Health, Part C*, *27*, 120–139. https://doi.org/10.1080/10590500902885684

Veen, T., Borge, T., Griffith, S. C., Saetre, G.-P., Bures, S., Gustafsson, L., & Sheldon, B. C. (2001). Hybridization and adaptive mate choice in flycatchers. *Nature*, *411*, 45–50. https://doi.org/10.1038/35075000

Wang, S., Ore, M. J., Mikkelsen, E. K., Lee-Yaw, J., Toews, D. P. L., Rohwer, S., & Irwin, D. (2021). Signatures of mitonuclear coevolution in a warbler species complex. *Nature Communications*, *12*, 1–11. https://doi.org/10.1101/2020.04.06.028506

Willett, C. S. (2012). Quantifying the elevation of mitochondrial DNA evolutionary substitution rates over nuclear rates in the intertidal copepod *Tigriopus californicus*. *Journal of Molecular Evolution*, *74*, 310–318. https://doi.org/10.1007/s00239-012-9508-1

Wolff, J. N., Ladoukakis, E. D., Enriquez, J. A., & Dowling, D. K. (2014). Mitonuclear interactions: Evolutionary consequences over multiple biological scales. *Philosophical Transactions of the Royal Society, B: Biological Sciences*, *369*, 20130443. https://doi.org/10.1098/rstb.2013.0443

SUPPORTING INFORMATION

Additional supporting information can be found online in the Supporting Information section at the end of this article.

How to cite this article: McDiarmid, C. S., Hooper, D. M., Stier, A., & Griffith, S. C. (2024). Mitonuclear interactions impact aerobic metabolism in hybrids and may explain mitonuclear discordance in young, naturally hybridizing bird lineages. *Molecular Ecology*, *00*, e17374. https://doi.org/10.1111/mec.17374